Nonuniversal scaling behavior of Barkhausen noise

Bosiljka Tadić*
Jožef Stefan Institute, University of Ljubljana, P.O. Box 3000, 1001-Ljubljana, Slovenia

We simulate Barkhausen avalanches on fractal clusters in a two-dimensional diluted Ising ferromagnet with an effective Gaussian random field. We vary the concentration of defect sites c and find a scaling region for moderate disorder, where the distribution of avalanche sizes has the form $D(s,c,L) = s^{-(1+\tau(c))}\mathcal{D}(sL^{-D_s(c)})$. The exponents $\tau(c)$ for size and $\alpha(c)$ for length distribution, and the fractal dimension of avalanches $D_s(c)$ satisfy the scaling relation $D_s(c)\tau(c) = \alpha(c)$. For fixed disorder the exponents vary with driving rate in agreement with experiments on amorphous Si-Fe alloys.

arXiv:cond-mat/9609050v1 5 Sep 1996

Barkhausen noise (BN) occurs at low temperatures when a *disordered* ferromagnetic sample is slowly driven by the external magnetic field. A small ramp in the field triggers one domain, and the perturbation spreads to the neighboring domains producing an avalanche, which manifests itself as a series of jumps in the magnetization as the system passes from one metastable state to another. Hysteresis in the field-magnetization plane is inherent to these processes. If the field is ramped up and down close to the coercive field of the sample, the avalanches show a broad distribution of sizes, although the triggering mechanisms are strictly local and fully deterministic. The avalanche-like dynamics is controlled by the spatial distribution of quenched-in defects of various types, and is not influenced by the thermal fluctuations (as long as the system is below its ordering temperature).

Besides its practical applications [1], Barkhausen noise has been studied both experimentally [2–8] and theoretically [4,9–13] as an interesting example of collective dynamical behavior far from equilibrium. Recent experimental studies of BN were made on amorphous alloys such as metglass 2605S-2 and alumel [2], metglass 2606TCA [3], VITROVAC 6025X [4], and on Fe-Ni-Co [5,6] and Si-Fe [6–8] alloys. Numerous data collected in these and other experiments show that the power spectrum decays with frequency as $\sim \omega^{-\phi}$ ($1.5 \leq \phi \leq 2$) and the distributions of size, duration, and energy associated with Barkhausen jumps exhibit a power-law behavior over a few decades with a cutoff. More detailed analysis reveals [4] that the measured critical exponents for various distributions obey certain scaling relations, which are also derived in Ref. [4] assuming a definite type of the elementary pulse.

Experiments were typically done on one sample and no special care was taken in controlling the strength (and type) of disorder, which is responsible for avalanche-like dynamics. Other details which influence the statistics of BN were studied. In particular, it was found in Ref. [8] that in 1.8% Si-Fe alloy the exponents characterizing the distributions of size and duration of Barkhausen pulses appear to vary linearly with the driving rate of the external field. Urbach *et al.* [5] studied the importance of demagnetizing effects.

The dynamics of field-driven random ferromagnets at zero temperature has been studied by numerical simulations using Ising model with random fields (RFIM) [9,10] and with random bonds of the spin-glass type (RBIM) [12,13]. It has been recognized that in both cases a critical level of disorder exists at which the response to the external field becomes slow, with a broad distribution of avalanche sizes. This disorder-driven phase transition has been reported to have unusually large critical region—50% above the critical point—in the case of 3-dimensional RFIM [10].

In the present work we would like to point out the relevance of another type of defects to the scaling behavior of BN. In magnetic systems random fields are generated on a semimacroscopic scale by other types of disorder (i.e., random site or random bond defects) when the system is placed in an external magnetic field [14]. At the asymptotic thermally driven phase transition random fields dominate, leading to a new universality class of (equilibrium) phase transitions [15]. However, far from equilibrium where the Barkhausen noise is produced, the impurities of this type may still be relevant and are competing with the random fields in the pinning of domain boundaries. In particular, in the case of Si-Fe alloys the sample is diluted by nonmagnetic ions, whereas in the case of Fe-Ni-Co alloys and metglass samples the type of defects can be described by the random anisotropy and random-bond models, respectively.

We consider the diluted ferromagnetic Ising model with concentration c of empty (i.e., zero spin) sites, and add a small Gaussian random field with variance f at each occupied site. It should be stressed that our model differs from the ones considered in Refs. [9–13] in two crucial aspects: (a) There is a larger parameter space in the (c,f)-plane, where the scaling behavior of the avalanches could emerge, and a well defined percolation threshold along the c-axis; (b) For $c \neq 0$ the avalanches contribut-

ing to Barkhausen noise develop on *noncompact clusters* of spins (see Fig. 1), the compactness of which is tuned via the parameter c. This leads to new prominent features of BN in diluted ferromagnets [16].

We start with a (coarse-grained) Ising model

$$\mathcal{H} = -\sum_{i,j} J_{ij} S_i S_j - \sum_i (h_i + H) S_i \equiv -\sum_i h_i^{loc} S_i \quad (1)$$

where $S_i = \pm 1$ and the interactions are $J_{ij} = J_0$ between nearst neighbor occupied sites, and $J_{ij} = 0$ if at least one site is a defect. We use a 2-dimensional square lattice with a fraction c of randomly distributed defect (i.e., $S_i = 0$) sites and periodic boundary conditions. As already mentioned, the local random fields h_i are generated on a semimacroscopic scale. We assume Gaussian distributed random fields with zero mean and variance f at each occupied site. The disorder is considered as quenched.

The system is driven by small ramps of the external field ΔH starting from a strong negative field $-H_{max}$ (for practical reasons $H_{max} \leq 4$). Parallel updating of spin states is applied according to the rule $S_i(t+1) =$ sgn $h_i^{loc}(t)$. For each rump of the external field the system is updated as long as there are no more unaligned spins. Clusters of flipped spins are monitored (an example is shown in Fig. 1 [17]) and the distribution of cluster sizes $D(s)$ is determined. The distribution is integrated over the whole hysteresis loop and averaged over total number of samples, ranging up to 400. We first show the results for a fixed driving rate $\delta h \equiv \Delta H / H_{max} = 0.01$.

In Fig. 2 the integrated probability distribution $D(s)$ of avalanches of size s or larger is shown for fixed random-field variance $f = 0.5$ and for few values of concentration c (varied along the dashed line on the phase diagram in Fig. 3). For very weak disorder close to the zero-temperature ferromagnetic fixed point (lower right corner in Fig. 3) the system is ordered and the external field flips the magnetization via a first order phase transition. Consequently, the hysteresis loop is rectangular and the integrated probability distribution shows zero slope (top curve in Fig. 2). At fixed $f = 0.5$ a finite slope appears first for $c \approx 0.05$, increasing gradually with c in the range $0.05 < c < 0.35$. Assuming

$$D(s) \sim s^{-\tau(c)} \quad (2)$$

and fitting the straight sections of the lines in Fig. 2 to Eq. (2), we determine the exponent $\tau(c)$ for $0.05 \leq c \leq 0.3$. We find that the exponent [18] $1 + \tau(c)$ varies from 1.155 ± 0.002 at $c = 0.05$ to 1.373 ± 0.001 at $c = 0.3$ (see inset to Fig. 1). It should be noted that the loss of the power-law behavior at a finite cutoff size is not exponential, but rather a stretched exponential with a c-dependent exponent (see also Ref. [4]).

In order to study the cutoff systematically, we varied the size of the lattice L at several fixed values of c. For the integrated probability distribution $D(s, c, L)$ the following scaling form is appropriate [19]

$$D(s, c, L) = \ell^{-\alpha} D(s\ell^{-D_s}, c\ell^{\lambda_c}, \ell^{-1} L) \, , \quad (3)$$

where α is the scaling exponent for the probability distribution of avalanches of length ℓ or longer, and D_s is the fractal dimension of avalanches (not to be confused with the fractal dimension of percolation clusters). The exponent λ_c is associated with the presence of defects. If the scaling function on the right hand side of Eq. (3) depends explicitly on $c\ell^{\lambda_c}$ with $\lambda_c \geq 0$, the criticality (and the associated power-law behavior) could be maintained only if the disorder is kept at a critical value, say, c_0, i.e., we are dealing with a (nonequilibrium) phase transition. For $c \neq c_0$ the system is subcritical and the coherence length should be specified as a function of disorder $\xi(c - c_0)$. On the other hand, the parameter c may appear implicitly via tuning of the exponents α and D_s in (3), while the simple finite-size scaling form remains valid. Our numerical data suggest that this is the case with Barkhausen avalanches for the range of concentrations in the interior region between lines (*i*) and (*ii*) (see Fig. 3). We find that the following scaling form is satisfied [20]

$$D(s, c, L) = L^{-\alpha(c)} \mathcal{D}(s L^{-D_s(c)}) \, . \quad (4)$$

By fitting the data for $L = 100$, 200, and 300 to the expression (4) we determine the exponent $\alpha(c)$ and the fractal dimension of avalanches $D_s(c)$ for several values of c (and f) in the region II. The results are also shown in the inset to Fig. 1 as a function of c for fixed $f = 0.5$. For each value of f a distinct family of curves is found. For instance, the finite-size scaling fit which is shown in Fig. 4 is obtained at the point $c = 0.1$, $f = 1$ (marked by $\star$ on the phase diagram), leading to the exponents $1 + \alpha = 1.54 \pm 0.02$ and $D_s = 1.98 \pm 0.02$, whereas at the same point we find $\tau = 1.294 \pm 0.003$. By comparing the scaling fits for different c further c-dependence of the scaling function in Eq. (4) of the form $\mathcal{D}(x) \sim x^{-\phi(c)}$ for $x \to 0$ was found, with numerical values of $\phi(c)$ close to $\tau(c)$.

The scaling region is further characterized by the following scaling relation [21]

$$\alpha(c) = \tau(c) \; D_s(c) \, , \quad (5)$$

which follows from (4) by choosing $s L^{-D_s} \approx 1$ and comparing to (2). It should be stressed that numerical values of the exponents obtained above by the power-law and finite-size scaling fits satisfy (within numerical error) the scaling relation (5) for several distinct values of c in the region II (cf. inset to Fig. 1).

In the critical region close to the transition line $c_0(f)$ (line *(i)* in Fig. 3) the finite-size scaling form (4) fails. Instead, a more general expression (3) with c-dependent coherence length is more appropriate, similar to the analysis in Refs. [10,13]. According to our results, the width

δc of the critical region in the direction of the c-axis is rather small $\delta c<0.05$, in contrast to the $c = 0$ case along f-axis, where the fits to the simple scaling form (4) are not satisfactory in a wide range of f. This indicates that the scaling and nonuniversality in the region II are closely related to the structure of the underlying spin clusters for $c \neq 0$ [22].

The scaling region defined via Eqs. (4) and (5) is also bounded from the side of strong disorder by the line $c^\star(f)$ (line *(ii)* in Fig. 3), which ends on the c-axis at the percolation threshold $c^\star(0) = 0.395$. Above this line the power-law is practically lost and strong disorder prevents formation of system-size avalanches (cf. the two lower curves in Fig. 2). We expect that in this region the self-similarity persists only on a finite scale $\xi_s(c) \ll L$, with

$$D(s, c, L) = s^{-\tau^\star} \mathcal{D}(s/\xi_s(c), sL^{-D_s^\star}) \ , \qquad (6)$$

similar to a subcritical cellular automaton [23]. Here the exponents $\tau^\star$ and $D_s^\star$ are referring to the transition point $c^\star(f)$, and the c-dependent correlation length is expected to behave as $\xi_s(c-c^\star) \sim (c-c^\star)^{-D_s^\star}$ [23]. More detailed analysis of both critical regions as well as the precise location of the transition lines $c_0(f)$ and $c^\star(f)$ is left for a future study.

By varying the driving rate δh at fixed disorder the distributions $D(s, \delta h)$ appear to have different slopes. For larger δh we find smaller exponents, for instance, at c =0.2, f = 0.5 the exponent $1+\tau$ =1.2904 $\pm$ 0.0015 found with the driving rate δh =0.01, becomes 1.2575 ± 0.0017 for $\delta h = 0.015$, and 1.239 ± 0.002 for $\delta h = 0.02$. Larger δh overdrives weaker pinning centers thus rendering the occurrence of larger avalanches more probable. This picture is in agreement with the experimental results on 1.8% Si-Fe alloy [8].

We have demonstrated that Barkhausen noise in *diluted* ferromagnetic samples at low temperatures depends on a variety of physical parameters which can be controlled experimentally, such as strength of disorder and the applied driving rate. The comparison with experiments on 1.8% Si-Fe alloy [8] where the driving rate was varied, is promising. Our numerical data suggest that a more complex behavior emerges when the degree of disorder is varied. This includes a nonequilibrium phase transition at critical disorder $c_0(f)$ and a true scaling region with nonuniversal exponents. Further studies, both theoretical and experimental, will help elucidate the general question of conditions that result in the breakdown of universality.

I would like to thank Professor Sava Milošević for stimulating discussions. This work was supported in part by the Ministry of Science and Technology of the Republic of Slovenia and by bilateral Slovene-German Project No. 1B0A6C.

* Electronic address: Bosiljka.Tadic@ijs.si

1 See L.B. Sipahi, J. Appl. Phys. **75**, 6978 (1994) and references therein; L.B. Sipahi, R.M. Govindaraju, and D.C. Jiles, *ibid* **75**, 6981 (1994).

2 P.J. Cote and L.V. Meisel, Phys. Rev. Lett. **67**, 1334 (1991); L.V. Meisel and P.J. Cote Phys. Rev. B **46**, 10822 (1992).

3 K. P. O'Brien and M.B. Weissman, Phys. Rev. E **50**, 3446 (1994).

4 Dj. Spasojević, S. Bukvić, S. Milošević, and H. E. Stanley, preprint.

5 J. S. Urbach, R. C. Madison, and J. T. Markert, Phys. Rev. Lett. **75**, 276 (1995).

6 O. Geoffroy and J. L. Portteseil, J. Magn. Magnetic Mat. **133**, 1 (1994); *ibid.* **97**, 198 (1991).

7 B. Alessandro, C. Beatrice, G. Bertotti, and A. Montorsi, J. Appl. Phys. **68**, 2908 (1990); C. Beatrice and G. Bertotti, J. Magn. Magnetic Mat. **104-107**, 324 (1992).

8 G. Bertotti, G. Durin, and A. Magni, J. Appl. Phys. **75**, 5490 (1994); G. Durin, and A. Magni, in *Fractal Reviews in the Natural and Applied Sciences*, p. 35, edited by M. Novak, Chapman & Hall, London (1995).

9 J. P. Sethna, K. Dahmen, S. Kartha, J. A. Krumhansl, B. W. Roberts, and D. Shore, Phys. Rev. Lett. **70**, 3347 (1993); K. Dahmen, S. Kartha, J. A. Krumhansl, and B. W. Roberts, J. Appl. Phys. **75**, 5946 (1994).

10 O. Perković, K. Dahmen, and J. P. Sethna, Phys. Rev. Lett. **75**, 4528 (1995).

11 J. V. Andersen and O. G. Mouritsen, Phys. Rev. A **45**, R5331 (1992).

12 C. M. Coram, A. E. Jacobs, and N. Heining, Phys. Rev. B **40**, 6992 (1989).

13 E. Vives and A. Planes, Phys. Rev. B **50**, 3839 (1994).

14 J. Imry and S.-k Ma, Phys. Rev. Lett. **35**, 1399 (1975).

15 See for instance G. Grinstein, Phys. Rev. Lett. (1976).

16 Recently the importance of this type of defects for magnetization avalanches in site-diluted metamagnet $Fe_xMg_{1-x}Cl_2$ was demonstrated in J. Kushauer, R. van Bentum, W. Kleemann, and D. Bertrand, Phys. Rev. B **53**, 11647 (1996).

17 I am grateful to Dr. Uli Nowak for his assistance in producing this picture.

18 Notice that our $1 + \tau(c)$ corresponds to measured exponent τ_{exp} of the probability distribution of sizes.

19 B. Tadić and R. Ramaswamy, Physica A **224**, 188 (1996); and cond-mat/9602092.

20 Apart from the c-dependence of the exponents, the same scaling form applies to the self-organizing cellular automata (SOC) studied by P.Bak, C. Tang, and K. Wiesenfeld, Phys. Rev. Lett. **59**, 381 (1987); Phys. Rev. A **38**, 364 (1988), and L.P. Kadanoff, S.R. Nagel, L. Wu, and M. Zhou, Phys. Rev. A **39**, 6524 (1989). An example of SOC with parameter-dependent exponents and a phase transition is studied in S. Lübeck, B. Tadić, and K.D. Usadel, Phys. Rev. E **53**, 2182 (1996).

21 This scaling relation (among others) was derived in Ref. [4] by assuming the elementary signal of the form $m(t) =$

$t^{\gamma-1}g(t/T)$. It should be noticed that our exponents are defined for the integrated distributions.

[22] Nonuniversality was also found in the self-afine asperity model of earthquakes in V. De Rubeis, Hallgass, V. Loretto, G. Paladin, L. Pietronero, and P. Tosi, preprint.

[23] See Ref. [19] and B. Tadić, U. Nowak, K.D. Usadel, R. Ramaswamy, and S. Padlewski, Phys. Rev. A **45**, 8536 (1992) for analysis of the subcritical CA, where $\xi_s(c) \sim c^{-D_s}$.

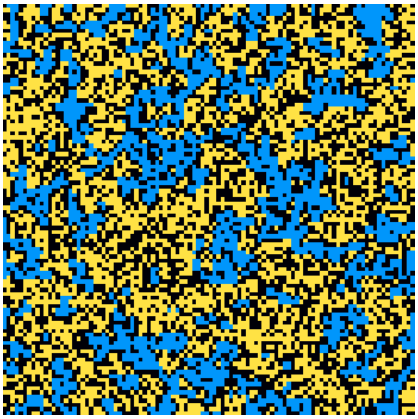

FIG. 1. Fractal cluster of connected spins close to the percolation threshold with areas of up spins (bright) and down spins (gray). Nonmagnetic defects are shown as dark points.

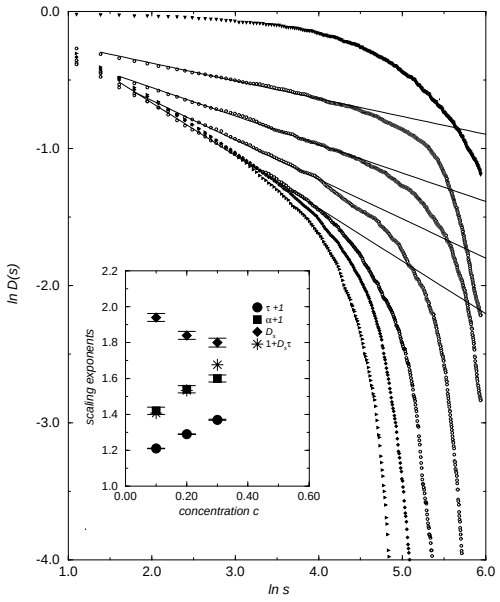

FIG. 2. Double logarithmic plot of the integrated distribution of size $D(s, c)$ vs. size s of avalanches for fixed lattice size L =100 and f = 0.5 and for various values of concentration c= 0.0, 0.05, 0.1, 0.2, 0.3, 0.35, and 0.4 (from top to bottom), normalized to the first point. Inset: Exponents of distributions of size $1 + \tau$, and length $1 + \alpha$, and fractal dimension D_s of avalanches plotted vs. c for fixed f=0.5 in the scaling region. Also plotted is $1 + D_s\ \tau$.

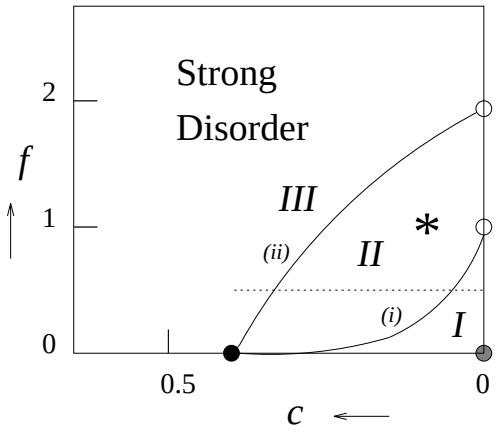

FIG. 3. Schematic phase diagram showing (I) region of 1st order phase transition, (II) scaling region, and (III) region of strong disorder. The system ceases to percolate along the line (ii), while a nonequilibrium phase transition in the universality class of RFIM occurs along the line (i). Results of Fig 2 are obtained by varying concentration c along the dashed line. The distributions in Fig. 4 are calculated at the point marked by $\star$.

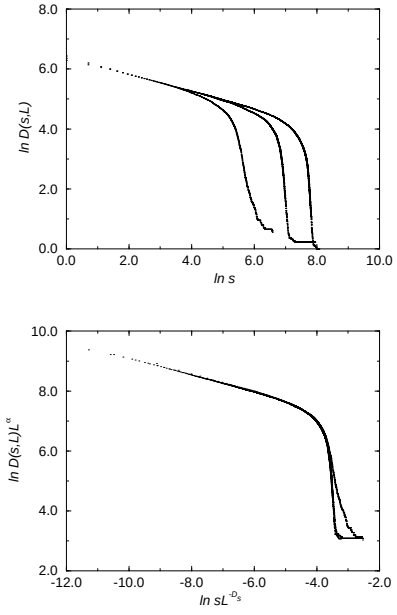

FIG. 4. Double logarithmic plot of the integrated distribution of size $D(s, c, L)$ vs. s for fixed c =0.1 and f =1.0 and three different values of lattice sizes L =100, 200, and 300 (top) and its finite-size scaling plot according to Eq. (4) (bottom).